

Thermal and Hadrochemical Equilibration in Nucleus-Nucleus Collisions at the SPS

P. Braun-Munzinger, J. Stachel, J. P. Wessels, and N. Xu*

Department of Physics

State University of New York at Stony Brook

Stony Brook, New York 11794 - 3800

(Sep. 22, 1995)

Abstract

The currently available set of hadron abundances at the SPS for central S + Au(W,Pb) collisions is compared to predictions from a scenario assuming local thermal and hadrochemical equilibrium. The data are consistent with a freeze-out temperature $T = 160 - 170$ MeV. Spectra are consistent with this temperature range and a moderate transverse expansion. The freeze-out points at the AGS and SPS are found to be close to the phase boundary between a hadron gas and an ideal quark-gluon phase.

Studies of ultra-relativistic nucleus-nucleus collisions in fixed target experiments at the BNL AGS and CERN SPS investigate hadronic matter at extreme density. Nuclei at the AGS are found to stop each other completely in the c.m. frame, while at the SPS an onset of transparency is observed for S+A collisions [1]. It has been predicted [2] that the longest lived systems with high density are produced somewhere between AGS and SPS energies. Hadronic cascade models yield densities in the interior of the colliding nuclei up to ten times normal nuclear matter density [3]. An intriguing possibility is that the phase boundary to quark matter is crossed in these collisions. For zero net baryon density the transition

temperature resulting from numerical simulations of QCD on a lattice is 150 ± 10 MeV [4]. A first order transition can be constructed for finite baryon density or non-zero up/down quark chemical potential between an ideal hadron gas and an ideal quark-gluon gas and the result will be shown below. We will first address the question to what extent one is allowed to actually talk about a phase in the thermodynamic sense. The question is whether the time scale is long enough and/or the collisions are frequent enough for the system to equilibrate before it breaks up (“freezes out”) into the final state hadrons. Present data are now detailed enough to address whether the system is in equilibrium at freeze-out.

Early data on global observables were seen [5] as indicative of a system with a temperature in the vicinity of 150 MeV, in local equilibrium but expanding longitudinally. Since then an extensive set of data on hadronic abundances and spectral distributions has become available for silicon and sulphur induced reactions and the hypothesis of thermal as well as hadrochemical equilibrium has been addressed by several authors [6–12]. In particular, in [10] an impressive and complete survey is given of theoretical techniques and their applicability to interpret data. For the AGS we have shown recently [11] that the complete set of hadron abundances is consistent with a system in equilibrium at a temperature in the range 120 - 140 MeV, a baryon chemical potential of 540 MeV, and strangeness in equilibrium with up/down flavors. The system appears to be in local equilibrium with an overall longitudinal and transverse expansion with average velocities of $\langle \beta_l \rangle = 0.52$ and $\langle \beta_t \rangle = 0.39 - 0.33$. Here we will use the same approach to test whether data at SPS energies are consistent with hadrochemical equilibrium as well.

We use for the present analysis the complete set of data now available from the different experiments. Previous studies often concentrated largely on the abundances of strange and multiply strange baryons, in part by choice and in part because some of the relevant nonstrange hadron and meson abundances were not available at the time. This approach yields significant discrepancies between model predictions and data when the most abundantly produced particles, pions, are considered, as was already noted by Redlich et al. [7]. Further, we will use data integrated over the maximum available range of rapidity and

transverse momentum since flow effects can severely distort relative hadron abundances at a given rapidity and transverse momentum. Similar to [6,7] we will investigate only the case of complete strangeness saturation instead of allowing an additional free parameter to govern abundances of strange hadrons as in [8–10,12]. In addition to comparing relative hadron abundances to the data we will also compare the absolute pion density from the thermal model to an estimate obtained from the experimental data.

The basic assumption of our thermal model is that in every local restframe the system is described by a grand canonical ensemble of fermions and bosons in equilibrium at (freeze-out) temperature T . For an infinite volume the particle number densities are given as integrals over particle momentum p :

$$\rho_i^0 = \frac{g_i}{2\pi^2} \int_0^\infty \frac{p^2 dp}{\exp[(E_i - \mu_b B_i - \mu_s S_i)/T] \pm 1} \quad (1)$$

where g_i is the spin-isospin degeneracy of particle i , E_i , B_i and S_i are its total energy in the local rest frame, baryon number and strangeness, and μ_b and μ_s are the baryon and strangeness chemical potentials (unless otherwise noted $\hbar = c = 1$). Energy density ϵ_i^0 , pressure P_i^0 , and entropy density σ_i^0 for a given species are obtained by evaluating equation 1 above with an additional factor of E_i , $p^2/(3E_i)$, and $(p^2/(3E_i) - \mu_i + E_i)/T$ in the integrand, respectively.

For a system of finite size the integrand in equation (1) has to be multiplied by a correction factor [13]. For an estimate of this correction we assume a spherical volume with radius R giving a correction factor

$$f = 1 - \frac{3\pi}{4pR} + \frac{1}{(pR)^2}. \quad (2)$$

To approximately account for the volume taken up by baryons we apply an excluded volume correction to the partition function,

$$\ln Z_i = \frac{\ln Z_i^0}{1 + \sum_j V_j \rho_j^0} \quad (3)$$

where V_j is the volume occupied by an individual baryon and the sum extends over all baryons; we use a sharp sphere volume with radius 0.8 fm for all baryons. The excluded vol-

ume correction for the pressure takes the same form as eq. 3; to correct the entropy, particle, and energy densities the appropriate derivatives of the correction factor with respect to temperature and/or chemical potential have to be taken into account. This simple correction is appropriate for $\sum_j V_j \rho_j^0 \leq 0.5$, valid for the area of interest in this paper. More general (and much more involved) procedures are discussed in [14]. The finite size and excluded volume corrections are sizeable and affect the absolute densities and pressures, but ratios of particle yields or quantities such as the entropy/baryon are affected to a lesser extent.

For the comparison to SPS heavy ion data we include in the thermal model all known [15] baryons and mesons up to a mass of 2 and 1.5 GeV, respectively. We have checked that for $T \leq 180$ MeV higher mass mesons and baryons do not play an important role and lead to corrections of less than 5 % in the particle densities. The correction for feeding and decay is performed as in [11] using all known branching ratios [15] and symmetry and phase space arguments for unknown branching ratios. Unless an explicit number is quoted by the experiment, we assume a 50 % particle identification efficiency following weak decays.

The starting point for our thermal model calculations is to determine, for each temperature, that baryon chemical potential with which are best described experimental data reflecting the proton to pion ratio (first four rows in Table I). As in [11] the strangeness chemical potential is fixed by the strangeness neutrality condition. Best overall agreement with all data is obtained with $T = 160 - 170$ MeV, as shown in Table I where all currently available experimental data on particle ratios measured in central S + Au(W,Pb) collisions are compared to predictions of the thermal model. A graphic illustration of what drives the temperature in our freeze-out analysis can be seen in Figure 1, where predictions for those particle ratios that show, after our choice of μ_b , the largest temperature sensitivity are plotted *vs* T. Typical changes are about a factor 30 over the temperature range considered and good overall agreement with the data for these temperature sensitive ratios is obtained for $T = 160 - 170$ MeV and corresponding baryon chemical potentials of 170 - 180 MeV, respectively. Since we assume strangeness equilibration all other particle ratios, including those for strange and multi-strange hadrons, are then fixed. Inspection of Table I shows that

with these two parameters one can obtain a surprisingly good description of the available experimental data.

Most measured particle ratios are reproduced well within the errors, especially keeping in mind systematic errors and systematic acceptance effects as displayed e.g. in Table I by data for the same ratio from different experiments. Of the 27 measured ratios spanning a range of a factor 400 just three differ beyond statistical errors by 40-50 % and the only more serious discrepancy is the ratio $(\Omega^+ + \Omega^-)/(\Xi^+ + \Xi^-)$ which appears to be about a factor 2 different. Note, however, that there is no systematic indication that a separate parameter is needed to control strangeness abundance. At the same time, there are significant differences (up to a factor of four) in the ratios for the heavy ion reaction considered here as compared to nucleon nucleon data [30].

The freeze-out temperature resulting from our analysis is considerably lower than that proposed by [9] and [10] to describe data. Although in the latter a range of temperatures is considered, the finally proposed chemical freeze-out temperature is 190 MeV causing, as the authors note, a significant underprediction in the pion abundance as compared to data. The lower temperature is reassuring, because temperatures around 200 MeV will lead to absolute pion densities of 0.6-0.7/fm³ after excluded volume correction, *i.e.* even pions start to overlap significantly (as noted also in [10]). Furthermore, such a high freeze-out temperature would imply that freeze-out takes place well in the quark-gluon plasma region of the phase diagram (see below). In fact, experimental data on two-pion interferometry can be used to obtain an estimate of the pion density at freeze-out. We begin by noting that experimental $\pi^+\pi^+$ and $\pi^-\pi^-$ correlations are rather well described by a simulation using the cascade code RQMD [31]. Next we inspect the space-time history of particles in RQMD. Pions freeze out over an extended time in RQMD during which the source is expanding. To give a typical volume we quote here the size of the system at the average pion freeze-out time $t = 14$ fm/c. At mid-rapidity the distribution of positions transverse to the beam is Gaussian with standard deviation $\sigma_x = \sigma_y = 4.0$ fm, the longitudinal distribution for low transverse momenta ($p_t \leq 0.1$ GeV/c) has a standard deviation of $\sigma_z = 7.7$ fm. This corresponds to a

volume $V = (2\pi)^{3/2}\sigma_x\sigma_y\sigma_z = 1940 \text{ fm}^3$. The rapidity integrated multiplicity for negatively charged particles for central S+Au collisions has recently been reported by NA35 [17] and from their data we estimate that the total pion multiplicity in these collisions is about 510. Using the volume estimate just given one obtains a typical pion density at freeze-out $\rho_\pi \approx 0.27/\text{fm}^3$. This is rather close to the value of $0.30/\text{fm}^3$ obtained in the thermal model for $T = 160 \text{ MeV}$ and the above parameters. Other volume estimates, e.g. obtained by using the time averaged variances or the variances of the time integrated distributions, are larger, leading to lower freeze-out density estimates.

The entropy at freeze-out, when evaluated in the thermal model, is found to be large. For $T = 160$ and 170 MeV we obtain for the entropy per net baryon, which is equivalent to the entropy produced per incident nucleon, values of $S/(\bar{B}-\bar{B}) = 45.4$ and 36.7 , respectively.

The strange chemical potentials obtained for $T = 160$ (170) MeV and $\mu_b = 170$ (180) MeV are $\mu_s = 38.0$ (47.0) MeV . On the quark level this implies a strange quark chemical potential of $\mu_{qs} = \frac{1}{3}\mu_b - \mu_s = 18.6$ (13.0) MeV , much smaller than the strange quark mass. Obviously, for every temperature T there is one value of μ_b which, together with strangeness conservation, will yield $\mu_{qs} = 0$. In the present case the pion to nucleon ratio happens to be such that we are close to this situation. This situation arises in a purely hadronic picture and is not related to whether or not the system is in the quark-gluon plasma phase at freeze-out.

In order to test whether the transverse momentum spectra of the various hadrons are consistent with a temperature of 160 MeV and one common transverse flow velocity we use, as in our analysis for the AGS [11], the formalism developed in [32]. To minimize systematic uncertainties, we choose spectra of different particle species measured in the same experiment and close to mid-rapidity and we have made the comparison for three sets: pion, kaon, proton and deuteron spectra from NA44 [33], where a similar fit is also shown; spectra of kaons, lambdas and cascades from WA85 [28,24] shown together with the fit in Fig. 2; the η to pion ratio from WA80 [22]. All spectra are consistent with a temperature of 160 MeV and, for a linear dependence of the flow velocity on the radius of the system ($\alpha =$

1), an average transverse expansion velocity of $\langle\beta_t\rangle = 0.27$. Consistent results were reported by [32] for spectra from S+S collisions. This value is somewhat smaller than the range of 0.33 - 0.39 found at AGS energies [11].

To put the above determined freeze-out temperature and baryon chemical potential into perspective we have calculated the phase boundary between the hadron resonance gas and the quark-gluon plasma by equating the chemical potentials and the pressure in the hadronic phase, with those of an idealized phase of massless u,d quarks, s quarks with mass of 150 MeV, gluons, and a bag constant of $B = 262 \text{ MeV/fm}^3$. The resulting phase diagram is shown in Figure 3 along with the latent heat and baryon densities at the transition line. Interactions among the hadrons, which are neglected in our approach, are not expected to change this phase boundary by much [14] except possibly at high baryon density ($\mu_b > 1 \text{ GeV}$), *i.e.* far away from the freeze-out region. The freeze-out points determined from the present analysis and from that for AGS data [11] are shown by the filled circles in this diagram. Note that, with this scenario, the system at freeze-out, *i.e.* **after** expansion and cooling, is close to the phase boundary at both AGS and CERN energies.

We would like to thank M. Prakash and E. Shuryak for enlightening discussions. This work was supported in part by the National Science Foundation. One of us (J. P. W.) is supported by the A. v. Humboldt Foundation as a F. Lynen fellow.

* present address: P-25 MS D456, LANL, Los Alamos, NM 87545.

REFERENCES

- [1] J. Stachel and G. R. Young, *Annu. Rev. Nucl. Part. Sci.* **42**, 537(1992).
- [2] C.M. Hung and E.V. Shuryak, preprint hep-ph/9412360
- [3] H. Sorge, A. von Keitz, R. Mattiello, H. Stöcker, and W. Greiner, *Phys. Lett.* **B243**, 7(1990) and H. Sorge, R. Mattiello, H. Stöcker, and W. Greiner, *Phys. Lett.* **B271**, 37(1991).
- [4] C. DeTar, in Proc. “Lattice ’94”, *Nucl. Phys.* **B42** (Proc. Suppl.), 73(1995).
- [5] J. Stachel and P. Braun-Munzinger, *Phys. Lett.* **B216**, 1(1989).
- [6] J. Cleymans, H. Satz, E. Suhonen, and D. W. von Oertzen, *Phys. Lett.* **B242**, 111(1990); N. J. Davidson, H. G. Miller, R. M. Quick, and J. Cleymans, *Phys. Lett.* **B255**, 105(1991); N. J. Davidson, H. G. Miller, and D. W. von Oertzen, *Phys. Lett.* **B256**, 554(1991).
- [7] J. Cleymans and H. Satz, *Z. Physik* **C57**, 135(1993); K. Redlich, J. Cleymans, H. Satz, and E. Suhonen, *Nucl. Phys.* **A566**, 391c(1994).
- [8] J. Letessier, A. Tounsi, J. Rafelski, *Phys. Lett.* **B292**, 417(1992); J. Letessier, J. Rafelski, A. Tounsi, *Phys. Lett.* **B328**, 499(1994).
- [9] J. Rafelski, *Phys. Lett.* **B262**, 333(1991); J. Sollfrank, M. Gaździcki, U. Heinz, J. Rafelski, *Z. Phys.* **C61**, 659(1994).
- [10] U. Heinz, *Nucl. Phys.* **A566**, 205c(1994); J. Sollfrank and U. Heinz, preprint HU-TFT-95-27, to be published in *Quark Gluon Plasma 2*, R.C. Hwa, editor, World Scientific.
- [11] P. Braun-Munzinger, J. Stachel, J. P. Wessels, and N. Xu, *Phys. Lett.* **B344**, 43(1995).
- [12] A. D. Panagiotou, G. Mavromanolakis, J. Tzoulis, preprint.
- [13] H. R. Jaqama, A. Z. Mekjian, and L. Zamick, *Phys. Rev.* **C29**, 2067(1984), see also R.

- Balian and C. Bloch, *Ann. Phys.* **70**, 401(1970).
- [14] R. Venugopalan, and M. Prakash, *Nucl. Phys.* **A546**, 718(1992).
- [15] Particles and Fields, *Phys. Rev.* **D50**, 1173-1926 (1994).
- [16] M. Murray for the NA44 Coll., *Nucl. Phys.* **A566**, 515c(1994).
- [17] M. Gaździcki for the NA35 Coll., *Nucl. Phys.* **A590**, 197c(1995).
- [18] J. Mitchell for the NA35 Coll, *Nucl. Phys.* **A566**, 415c(1994).
- [19] A. Iyono et al., EMU05 Coll, *Nucl. Phys.* **A544**, 455c(1992); and data from EMU05 shown in R. Hołyński, *Nucl. Phys.* **A566**, 191c(1994).
- [20] J. Simon-Gillo et al., NA44 Coll., *Nucl. Phys.* **A590**, 483c(1995).
- [21] B. Jacak, NA44 Coll., in “Hot and Dense Nuclear Matter”, W. Greiner, H. Stöcker, and A. Gallmann, eds. (Plenum, New York,1994) p.607.
- [22] R. Albrecht et al., WA80 Coll., preprint, hep-ex/9507009, July 1995.
- [23] M. Massera for the Helios3 Coll., *Nucl. Phys.* **A590**, 93c(1995).
- [24] D. Di Bari for the WA85 Coll., *Nucl. Phys.* **A590**, 307c(1995).
- [25] T. Alber et al., NA35 Coll., *Z. Physik* **C64**, 195(1994).
- [26] D. Röhrich for the NA35 Coll., *Nucl. Phys.* **A566**, 35c(1994).
- [27] J. Günther for the NA35 Coll., *Nucl. Phys.* **A590**, 487c(1995).
- [28] S. Abatzis et al., WA85 Coll., *Phys. Lett.* **B270**, 123(1991) and *Nucl. Phys.* **A566**, 225c(1994).
- [29] E. Andersen for the NA36 Coll., *Nucl. Phys.* **A566**, 217c(1994).
- [30] M. Gaździcki and O. Hansen, *Nucl. Phys.* **A528**, 754(1991).

- [31] H. Bøggild et al., NA44 Coll., Phys. Lett. **B349**, 386(1995).
- [32] E. Schnedermann, J. Sollfrank, and U. Heinz, Phys. Rev. **C48**, 2462(1993); E. Schnedermann and U. Heinz, Phys. Rev. **C50**, 1675(1994).
- [33] J. Dodd for the NA44 Coll., Nucl. Phys. **A590**, 523c(1995).

TABLES

TABLE I. Particle ratios calculated in a thermal model for temperatures of 160 and 170 MeV, baryon chemical potential μ_b of 170 and 180 MeV and strangeness chemical potential μ_s of 38.0 and 47.0 MeV, in comparison to experimental data (with statistical errors in parentheses) for central collisions of 200 A GeV/c S + Au(W,Pb). For experimental data a p_t range is quoted when the lower limit is significantly larger than zero.

Particles	Thermal Model		Experimental Data			
	T(MeV)		exp. ratio	ref.	y	p_t
	160	170				
p/π^+	0.17	0.19	0.18(3)	NA44 [16],NA35 [17]	2.6-2.8	
pos-neg/neg	0.18	0.21	0.15(1)	NA35 [18]	4-5.8	
$p-\bar{p}$ /neg	0.13	0.14	0.15(2)	NA35 [26,17]	3.2-5.4	
pos-neg/pos+neg	0.084	0.094	0.088(7)	EMU05 [19]	2.3-3	
d/p	0.014	0.017	0.015(2)	NA44 [20]	1.8-2.5	
\bar{p} /p	0.13	0.14	0.12(2)	NA44 [21]	2.65-2.95	
\bar{p}/π^-	0.022	0.027	0.024(9)	NA44 [16],NA35 [17]	2.6-2.8	
η/π^0	0.12	0.12	0.15(2)	WA80 [22]	2.1-2.9	
$\phi/(\rho + \omega)$	0.11	0.12	0.080(20)	Helios3 [23]	≥ 3.5	
K^+/π^+	0.21	0.22				
$K^+ + K^- / K_s^0$	1.05	1.06	1.07(3)	WA85 [24]	2.5-3.0	1-2
K^+ / K^-	1.46	1.53	1.67(15)	WA85 [24]	2.3-3.0	> 0.9
K_s^0 / Λ	1.74	1.50	1.4(1)	WA85 [24]	2.5-3.0	1-2.5
	1.57 ^a	1.36 ^a	0.88(10)	NA35 [25]	3.5-5.5	
$K_s^0 / \bar{\Lambda}$	8.5	6.6	6.4(4)	WA85 [24]	2.5-3.0	1-2.5
	7.3 ^a	5.7 ^a	4.6(10)	NA35 [25]	3.5-5.5	
$\Lambda / (p-\bar{p})$	0.67	0.69	0.45(4)	NA35 [26]	3.25-5.25	
$\bar{\Lambda} / \bar{p}$	0.38	0.41	0.80(30)	NA35 [27]	3.25-5.0	
$\bar{\Lambda} / \Lambda$	0.20 ^b	0.23 ^b	0.20(1)	WA85 [28]	2.3-3.0	1.2-3
			0.207(12)	NA36 [29]	1.5-3.0	0.6-1.6
	0.22 ^a	0.24 ^a	0.19(4)	NA35 [25]	3.5-5.5	
Ξ^- / Λ	0.12 ^b	0.12 ^b	0.095(6)	WA85 [28]	2.3-5.0	1.2-3
			0.066(13)	NA36 [29]	1.5-2.5	0.8-1.8

$\Xi^+/\bar{\Lambda}$	0.20 ^b	0.21 ^b	0.21(2)	WA85 [28]	2.3-3.0	1.2-3
			0.127(22)	NA36 [29]	2.0-3.0	0.6-1.8
Ξ^-/Ξ^+	0.31	0.36	0.45(5)	WA85 [28]	2.3-3.0	1.2-3
			0.276(108)	NA36 [29]	2.0-2.5	0.8-1.8
$(\Omega^+ + \Omega^-)/(\Xi^+ + \Xi^-)$	0.17	0.19	0.8(4)	WA85 [24]	2.5-3.0	>1.6
\bar{d}/\bar{p}	.0015	.0018				

^aReconstruction efficiency $\epsilon = 1$ for particles from weak decays.

^b Yields of $\Lambda, \bar{\Lambda}$ corrected for feeding from Ξ .

FIGURES

FIG. 1. Ratios of baryon abundances that show a strong temperature dependence for a fixed pion to nucleon ratio as indicated in Table I. See text for details.

FIG. 2. Kaon, Lambda and Cascade spectra from WA85 [28,24] compared to thermal model calculations with $T = 160$ MeV and an average transverse expansion velocity of $\langle\beta_t\rangle = 0.27$ (solid lines).

FIG. 3. Phase boundary between a hadron gas and a quark-gluon plasma (top) as function of temperature and baryon chemical potential together with the freeze-out points for Si(S) + Au(W,Pb) collisions at AGS [11] and SPS (present paper) energies. Latent heat of the phase transition (middle) and baryon density in the hadron and quark-gluon phase at the phase boundary (bottom).

Figure 1

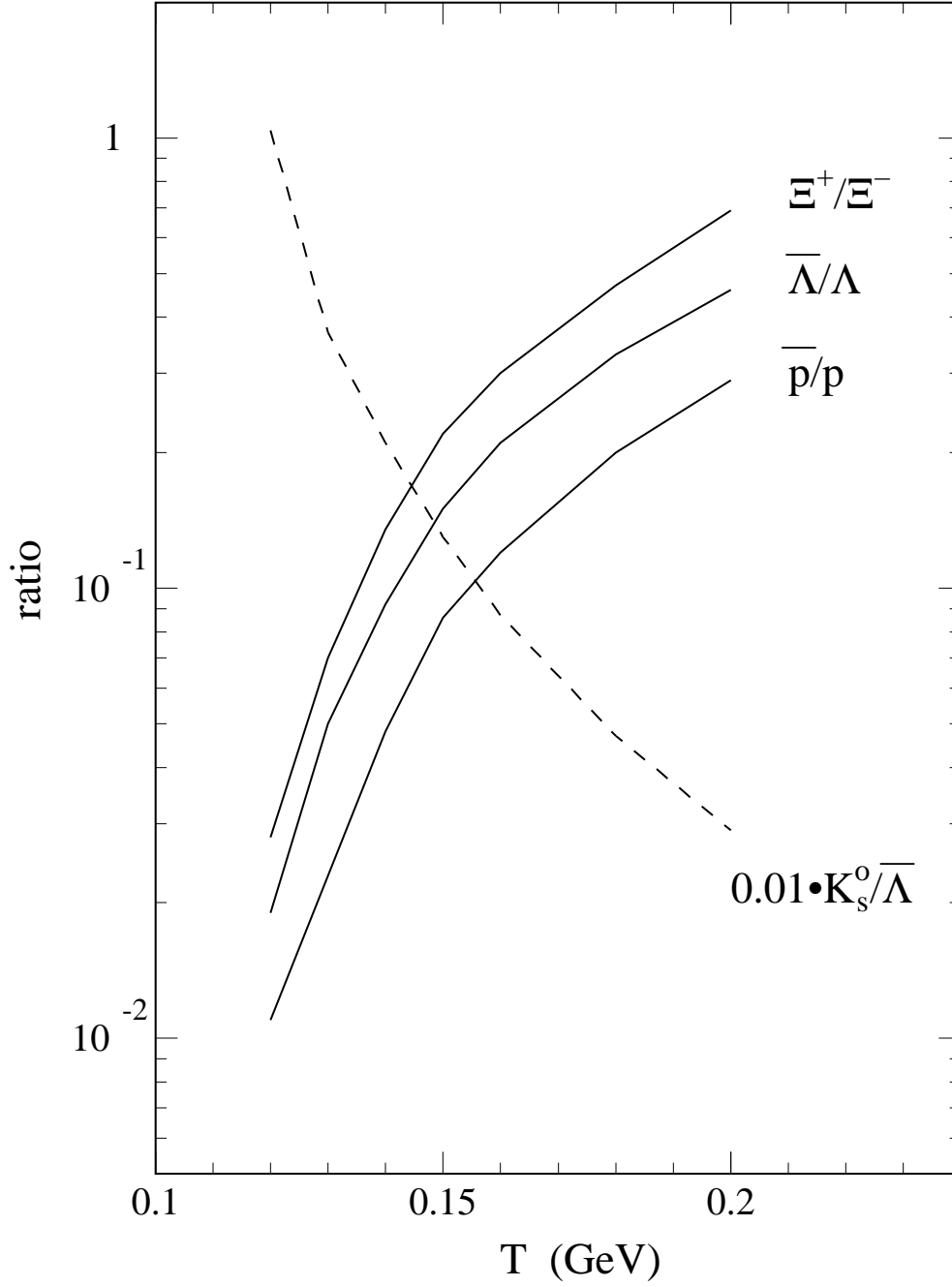


Figure 2

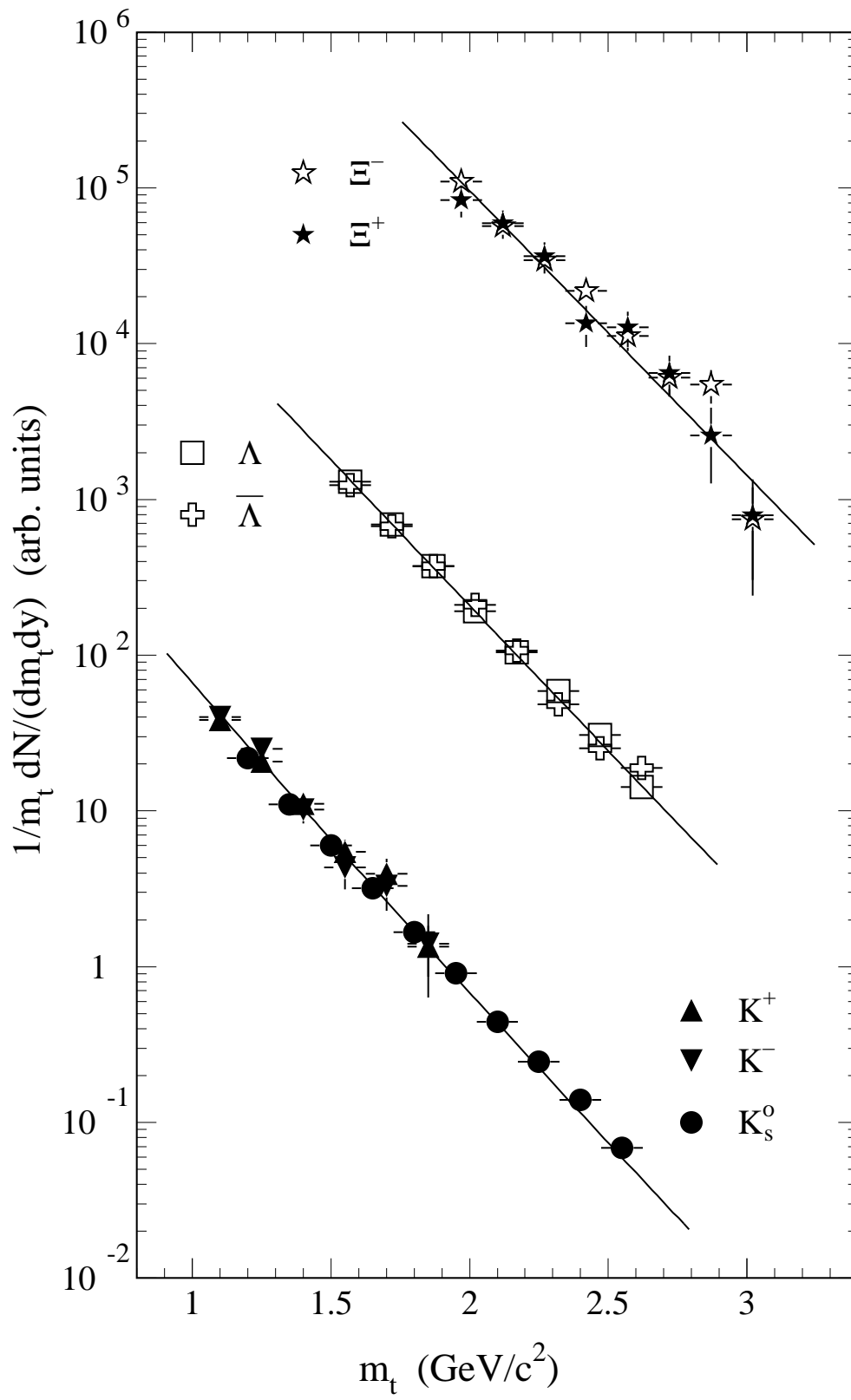


Figure 3

